Evaluation of FBMC Channel Estimation using multiple Auxiliary symbols for high throughput and low BER 5G and beyond communications

T. Padmavathi[1]*, Kusma Kumari Cheepurupalli[2], and R. Madhu[3]

***Abstract*—Filter Bank Multi-Carrier (FBMC) modulation has been recognized as a consistent contender and a possible successor for Orthogonal Frequency Division Multiplexing (OFDM) in 5G and beyond because of its outstanding spectral properties. The channel is assessed in FBMC using pilot-symbol aided channel estimation that provides robust estimates even for severe channel conditions. In the present work, neutralizing the imaginary interference at the pilot positions is focused while estimating the channel. To neutralize the imaginary interference, multiple auxiliary symbols have been proposed to enhance the throughput and channel capacity. The Iterative Minimum Mean Squared Error (IMMSE) cancellation scheme has been proposed to reduce the interference at the pilot and data positions. Transmission power, Bit Error Rate (BER) and throughput are computed for Filter Bank Multi Carrier (FBMC), OFDM and proven that better system performance is obtained for FBMC. The performance of channel estimation is evaluated through 5G standards and indicates that the usage of multiple auxiliary symbols per pilot leads to better throughput and low Bit Error Rate at low power transmission.**

***Index Terms*—Filter bank Multi Carrier, Auxiliary symbols, Imaginary interference, Bit Error Rate, Throughput, 5G and beyond Communications.**

I. INTRODUCTION

Cyclic Prefix - Orthogonal Frequency Division Multiplexing (CP-OFDM) is a noticeable transmission technique used in various wireless communication standards i.e 4G Long-Term Evolution (LTE) [1], Digital Audio and Video Broadcasting-terrestrial (DVB-T) [2], Wireless Local Area Networks (WLAN). In OFDM system, wideband frequency spectrum has divided into numerous parallel sub bands. One tap channel equalizer is adequate at the receiver because OFDM system is more robust to frequency selective channels. However, cyclic prefix insertion is required for CP-OFDM systems in order to get these benefits. However, cyclic prefix increases the redundancy in a time domain. Additionally, it must ensure the guard bands in the frequency domain to avoid excessive Out-of-Band (OOB) emission [3].

[1]* T. Padmavathi, [1]*Sr Asst professor, Department of Electronics and Communication Engineering, CVR College of Engineering, Ibrahimpatnam, India. (E-mail: padmatp41@gmail.com)

[2] Kusma Kumari Cheepurupalli, [2]Associate Professor, Department of Electronics and Communication Engineering, Gayatri Vidya Parishad College of Engineering (Autonomous), Visakhapatnam, India.
(E-mail: chkusumasrinivas@gvpce.ac.in)

[3] R. Madhu, [3]Assistant Professor, Department of Electronics and Communication Engineering, University College of Engineering Kakinada (A), JNTUK Kakinada, India. (E-mail: madhu_ramarkula@rediffmail.com)

DOI: 10.36244/ICJ.2024.2.4

Due to these redundant resources in the time domain and frequency domain, the spectral efficiency of CP-OFDM systems is reduced.

New modulation techniques are required to overcome these constraints Future wireless systems must accommodate a wide range of communication needs, such as enhance Mobile Broadband (eMBB) and Ultra-Reliable Low Latency communication (URLLC) [4], [5] and so on. New modulation techniques are required to overcome these constraints. Filter Bank Multi Carrier (FBMC) is a new waveform technique that has many advantages over OFDM as a contender for use of 5G communication systems. The only notable difference is the substitution of OFDM for a multi-carrier system based on filter banks at the transmitter and receiver, which increases bandwidth utilization. FBMC technology uses a good time-frequency prototype filter, which has many advantages such as low spectral side lobes, high spectrum efficiency, and frequency offset robustness [6]. However, because the system is not strictly orthogonal, imaginary interference exists, but this necessitates the estimation of channel coefficients in the complex domain.

In recent years, FBMC-Orthogonal Quadrature Amplitude Modulation (FBMC-OQAM) has been noticed as a strong contender due to its spectral features [7-8]. However, there are some drawbacks, such as less compatibility with Multiple-Input and Multiple-Output (MIMO) [9]. The real orthogonality is maintained by FBMC-OQAM systems only, but it suffers from inherent interference in the complex domain. As a result, conventional channel estimation approaches of OFDM systems are incompatible with FBMC-OQAM systems [10-12]. To resolve this issue, Lee.et.al proposed a single prototype filter based FBMC-QAM.[13]. However, for ideal channels the FBMC-QAM system with a single prototype filter does not guarantee orthogonality between adjacent subcarriers and symbol intervals. As a result, the FBMC-QAM system with a filter-based design does not meet orthogonality constraints in the complex domain [14].

For FBMC-QAM systems, a conventional scattered pilot assisted channel estimation approach is used.[15] In this work, a prototype filter with a well-localized spectrum and a higher self-Signal to Interference Ratio (SIR) is used. After receiving a signal, a proto-type filtering is implemented, and the channel is estimated at the pilot position using Least Squares (LS) approach. However, the interference is not canceled at the pilot symbols using the conventional channel estimation scheme. As a result, the performance of channel estimation reduced for frequency selective channels.

Several preamble-based schemes for Channel Estimation (CE) have been proposed. The Interference Approximation Method (IAM) [16] and in the literature Interference Cancellation Method (ICM) [17] are two well-known interference mitigation algorithms. They either reduce or exploit imaginary interference to improve CE performance. In [18], a novel preamble structure for FBMC systems was proposed in conjunction with these methods.

To estimate time and frequency for frequency selective channels, a Minimum Mean Squared Error (MMSE) channel estimation method is applied [19-20]. By using this method, clustered pilots are used and only one OFDM symbol is taken into consideration at a time. In FBMC, while estimating the channel with MMSE channel estimation, time-varying characteristics of the wireless channels are not considered. Many authors investigated the inherent interference of pilot symbols and proposed channel estimation algorithms for auxiliary symbols [21-22]. Unfortunately, transmitting additional symbols necessitates giving up certain time-frequency blocks, which reduces bandwidth efficiency. Furthermore, the result of [23] reveals that the auxiliary symbol scheme has an unsatisfactory Bit Error Rate (BER), implying that channel estimate accuracy is low.[24] presents a compressed sensing-based channel estimation strategy that takes the channel's sparsity into account while still beginning with the auxiliary symbol approach. To design an Inter-carrier Interference (ICI)-free structure over a doubly selective channel using the auxiliary symbol approach, [25-26] time-frequency blocks must be sacrificed. As a result, this system exhibits low spectral efficiency and inaccurate channel estimation.

Pilot Aided Channel Estimation (PACE) is considered as one of the best techniques for tracking the wireless channel characteristics. A single auxiliary symbol is allotted to each pilot in order to apply PACE in FBMC [27-28]. But compared to the data symbol power, this approach needs higher auxiliary symbol power. Instead of one auxiliary symbol, two are used to solve this problem. One auxiliary symbol is utilized in this estimation technique to minimize the Peak to Average Power Ratio (PAPR) and achieve the maximum channel capacity for a specific range of Signal to Noise Ratio (SNR). The other symbol is utilized to prevent more power offset with the expense of computational complexity.

In this work, a different approach is proposed in choosing the auxiliary pilot symbols to reduce the power offset, at the same time to enhance channel capacity for low SNR. A randomly generated coding matrix is also included for the selection of the auxiliary pilot symbols.

Filter Bank Multi Carrier System model

The limitations of OFDM can be eliminated in FBMC by including pulse shaping filter in both time and frequency domain. Consequently, FBMC systems have more spectral containment signals and offer more effective use of the radio resources where no CP is required.

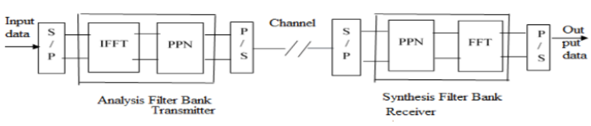

Figure 1. Transmitter and Receiver of FBMC System

In Filter Bank Multicarrier transmission shown in Figure.1. The transmitted signal from FBMC transmitter with data symbol $x_{l,k}$ and basis pulse $g_{l,k}(t)$ at l^{th} subcarrier position with time position k is given by

$$s(t) = \sum_{k=0}^{K-1} \sum_{l=0}^{L-1} g_{l,k}(t) x_{l,k}(t) \quad (1)$$

where L is the number of subcarriers and K is the number of multicarrier symbols with basis pulse. The basis pulse $g_{l,k}(t)$ is expressed as

$$g_{l,k}(t) = p(t-kT)e^{j2\pi lF(t-kT)}e^{j\theta_{l,k}} \quad (2)$$

The prototype filter basis pulse $p(t)$ shifted in the time and frequency domain is given in the Eq.2. The throughput of FBMC can be maximized by low frequency spacing F and time spacing T. Multi carrier system orthogonality requires a condition $TF \geq 1$ and basis pulse localization in both time and frequency domain. The requirement of prototype filter $(\theta l, k = 0)$ $p(t)$, frequency localization can be violated, because of CP in OFDM. In FBMC, Hermite polynomials $Hi(.)$ based basis pulse is employed. Because these polynomials produce great trade-off between time and frequency localization [29-30].

A different prototype filter $Rx(t)$ can be used at the receiver, so that the receiver basis pulses $q_{l,k(t)}$ can be expressed as in Eq.3

$$q_{l,k}(t) = P\ Rx(t-kT)e^{j2\pi lF(t-kT)}e^{j\theta_{l,k}} \quad (3)$$

To simplify the above analytical expression, the transmission system can be represented using a discrete time system model. The basis pulses are sampled with symbol rate $f_s = \frac{1}{\Delta t} = FN_{FFT}$ and obtains all the samples in large vector $g_{l,k} \in \mathbb{C}NX1$. $Q = [g_{0,0} \text{------} g_{L-1,K-1}]$ € $\mathbb{C}NXLK$ represent the receive basis pulse samples. In OFDM, the orthogonality denotes that $Q^H G = I_{L,K}$, whereas in FBMC, the real orthogonality condition maintains true if $\Re\{Q^H G\} = I_{L,K}$.

The received data symbol vector Y€ $\mathbb{C}LK\ X\ 1$ over time and frequency selective channel is represented as in Eq.4

$$Y = diag\{h\}Dx + n \quad (4)$$

with $D = Q^H HG$

The channel can be represented by a vector h€ $\mathbb{C}LKX1$ and complex Gaussian noise vector n is represented by a vector $n \sim N(0, P_n Q^H Q)$

II. Existing Pilot symbol channel estimation approach

The pilot symbols are known at the receiver before data transmission in pilot symbol channel estimation [31]. At the pilot position $(l,k) \in P$, the channel $h_{l,k}$ can be estimated using LS approach by dividing the received symbol $y_{l,k}$ with pilot symbol $x_{l,k}$. The estimate of channel at pilot position $h_p^{\wedge LS} \in C^{|PX1|}$ using one -tap channel is given by Eq.5

$$h_p^{\wedge LS} = diag(x_p)^{-1} y_p \quad (5)$$

Due to imaginary interference in FBMC, additional preprocessing becomes necessary. This can be done by precoding with help of Eq.6

$$X = cx \quad (6)$$

where the data symbol denoted by $\overline{x}$ and c is the precodingmatrix. The imaginary interference is cancelled at pilot position if the below Eq-7 is satisfied.

$$T\{q_p^H G\}Cx = 0 \quad (7)$$

Either Auxiliary Symbol Method [32] or Data spreading Approach can be used to frame precoding matrix C.

A. Proposed Auxiliary Pilot Symbol Approach

There are many symbols close to pilot symbols shown in Figure 2, resulting in imaginary interference. In the conventional technique, one of these symbols is used to cancel the imaginary interference [33].

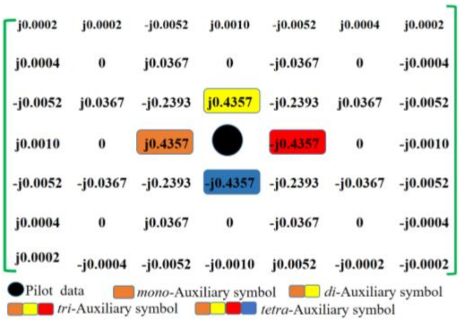

Figure 2: Selection of Auxiliary symbols close to the pilot symbol in the matrix

In order to cancel the imaginary interference, the neighbouring auxiliary pilot symbols are selected by using below Eq.8

$$X_p = [D_{P,P} \quad D_{P,D} \quad D_{P,A}] \begin{bmatrix} x_P \dots \dots \dots \\ x_D \dots \dots \dots \\ x_A \dots \dots \dots \end{bmatrix} \tag{8}$$

The vector $x_P \in R^{|P|X1}$represents all the elements of X at the pilot position. The same is applied to $x_D \in R^{|D|X1}$ at the data position & $x_A \in R^{|A|X1}$ at the auxiliary position. The row elements and column elements of D matrix forms the matrix $D_{P,D} \in C^{|P|X|D|}$ by taking pilot position and data position into account. The same is continued for $D_{P,P}$ and $D_{P,A}$.

Consider one auxiliary symbol per pilot, then $D_{P,A}$ represented by a diagonal matrix. From the elements of diagonal matrix shown in Figure. 2, the interference weight at auxiliary pilot position is 0.4357 is considered to compute the auxiliary pilot power offset K_A, and it is expressed using Eq.9[34].

$$K_A = \frac{P_A}{P_D} \tag{9}$$

where P_A is the power of auxiliary symbol, P_D is the power of data symbol. To cancel $N = 8$ closest interference symbols given in Figure.2. The auxiliary power offset given by

$$\frac{[4(0.2393)^2 + 3(0.4357)^2]}{(0.4357)^2} = 4.27$$

The auxiliary symbol must reimburse the imaginary interference from the adjacent symbols (without the auxiliary symbol), leading to an interference power of $(1 - 0.4357^2)$. Furthermore, the auxiliary symbol must be multiplied by $\frac{1}{0.4357}$ to compensate for the loss given by the interference weight. Thus, the auxiliary symbol power is $\frac{1-0.4357^2}{0.4357^2} = 4.21$ times higher than the data symbol power. In the proposed method it was observed that the auxiliary symbol power is reduced from 4.21 to 0.08 while increase from *mono* to *tetra* auxiliary symbol which is shown in Table.1.

TABLE I

AUXILIARY POWER OFFSET FOR INTERFERENCE WEIGHTS (ε=0.4357)

	mono-Auxiliary symbol	*di*-Auxiliary symbol	*tri*-Auxiliary symbol	*tetra*-Auxiliary symbol
$\frac{P_A}{P_D}$	$\frac{1-\varepsilon^2}{\varepsilon^2} = 4.21$	$\frac{1-2\varepsilon^2}{(2\varepsilon)^2} = 0.82$	$\frac{1-3\varepsilon^2}{(3\varepsilon)^2} = 0.25$	$\frac{1-4\varepsilon^2}{(4\varepsilon)^2} = 0.08$

With the increase in usage of auxiliary symbols, it is observed that a shortfall in data symbols. Even if there is a loss in data symbol, the throughput for certain range of Signal to Ratio (SNR) is not degraded. BER is one of the performance metrics which must be taken care of in channel estimation. While transmitting the data symbol and pilot symbol, channel estimation becomes complex due to the channel transfer function discontinuity at the edge of subcarriers. This is due to the estimation methods depending on an assumption that the channel delay taps are limited in time [35]. Even though the channel is estimated accurately, the resulting matrix multiplication is given in Eq.7 which is computationally complex.

The iterated MMSE Channel estimation method proposed in this paper works as follows:

Algorithm 1 Iterated MMSE Channel estimation

1. Compute transmission matrix with data given in Eq-2
2. Perform One-tap channel equalization followed by quantization then estimate
3. $x_{l,k}^{\wedge(0)} = Q\{\frac{y_{l,k}^{(0)}}{h_{l,k}^{\wedge(0)}}\}$, with $h^{\wedge(0)} = diag\{D^{\wedge(0)}\}$
4. Initialize the iteration with $i = 0$
5. Interference can be cancelled from the received signal.
6. $y^{(i+1)} = y - (D^{\sim(i)} - diag\left\{diag\{D^{\sim(i)}\}\right\})x^{\wedge(i)}$
7. Obtain channel estimation data matrix $D^{\wedge(i+1)}$ with less interference at pilot position.
8. Equalize the received signal with improved channel estimate and quantize, then obtain estimate of transmitted signal.
9. $x_{l,k}^{\wedge(i+1)} = Q\{\frac{y_{l,k}^{(i+1)}}{h_{l,k}^{\wedge(i+1)}}\}$
10. Consider $i = 0, 1, \dots \dots 4$ and repetition of step 4 to step 7.

where subscript $(.)^{(i)}$denotes i^{th}iteration step.

The modified MMSE channel estimation enhances accuracy by canceling the interference with the above method. The underlying correlation of channel matrix does not cancel the interference at the pilot positions because of nonlinearities in wireless channel. To overcome this problem, iteration step $i = 3$ *and* 4 are considered and interference is perfectly cancelled.

III. EXPERIMENTAL RESULTS

FBMC has lower side lobes and smaller guard bands resulting in higher spectral efficiency than OFDM. In order to achieve the advantages of FBMC and to enhance the performance of the proposed channel estimation method, LTE standards are considered to implement the system. This improvement is also evaluated by implementing FBMC with $1.4MHz$ LTE spectrum. The subcarrier spacing of $F = 15KHz$ is considered in FBMC like OFDM signal. Cyclic prefix length of $4.75\mu s$ and $K^{OFDM}(Number\ of\ symbols) = 14$, which results in the symbol duration as $1ms$ for OFDM signal, whereas FBMC allows to transmit $K^{OFDM}(Number\ of\ real\ symbols) = 30$ within the same symbol duration i.e $1ms$. Even though LTE occupies $1.4MHz$, OFDM only uses $L = 72$ subcarriers $(LF = 1.08MHz)$ whereas in FBMC, there are much lower sidelobes, the number of subcarriers is increased to $L = 87$ corresponds to $LF = 1.305MHz$.

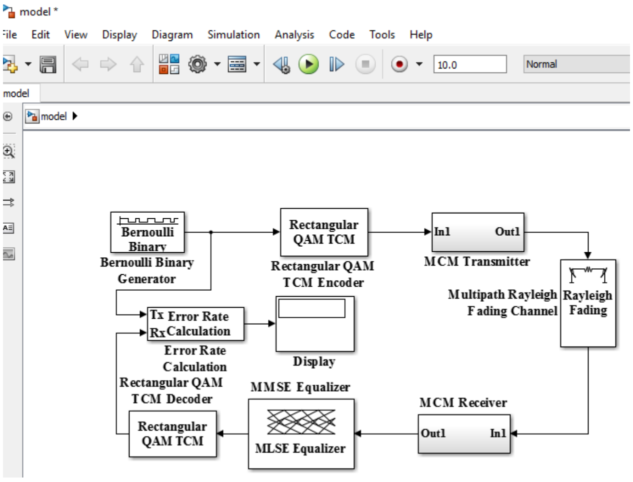

Figure. 3. Experimentation model for Throughput and BER

Transmission power

The pilot symbol pattern for FBMC is considered a diamond-shaped pattern, and the pilot density of |P| (KT LF) = 0:044 is chosen from the LTE standards. The data symbol power is the same as the pilot symbol power $P_P = P_D$. If the pilot power is increased by a factor of two, resulting in the same SNR for channel estimation (complex domain) and data transmission (real domain). The signal is transmitted with the 2.4955 GHz carrier through the Rayleigh fading channel to achieve several channel realizations. Modulation order, code rate, and turbo coding are taken from LTE standards to evaluate throughput. In turbo coding, while transmitting a signal the highest 15 Channel Quality Indicator (CQI) values, can be selected to get the highest throughput for all data bits.

To compare OFDM and FBMC, the same transmission power P_S is considered, and defined as:.

$$P_S = \frac{1}{KT}\int_{-\alpha}^{\alpha} E\{s(t)^2\} \tag{10}$$

The signal length in the time domain is given by KT and the transmitted signal $s(t)$ is given in Eq.1. For the same transmission power P_S, SNR of OFDM and FBMC is given by

$$SNR_{FBMC} = SNR_{OFDM}\frac{L^{OFDM}}{L^{FBMC}} \tag{11}$$

The SNR can be expressed as

$$SNR_{OFDM} = \frac{|D_{OFDM}|P_{D,OFDM}+|P_{OFDM}|P_{P,OFDM}}{L_{OFDM}K_{OFDM}P_n} \tag{12}$$

$$SNR_{FBMC} = \frac{|D_{FNA}|P_{D,FNA}+|P_{FNA}|P_{P,FNA}+|A_{FNA}|P_{A,FNA}}{L_{FBMC}K_{FBMC}\frac{P_n}{2}} \tag{13}$$

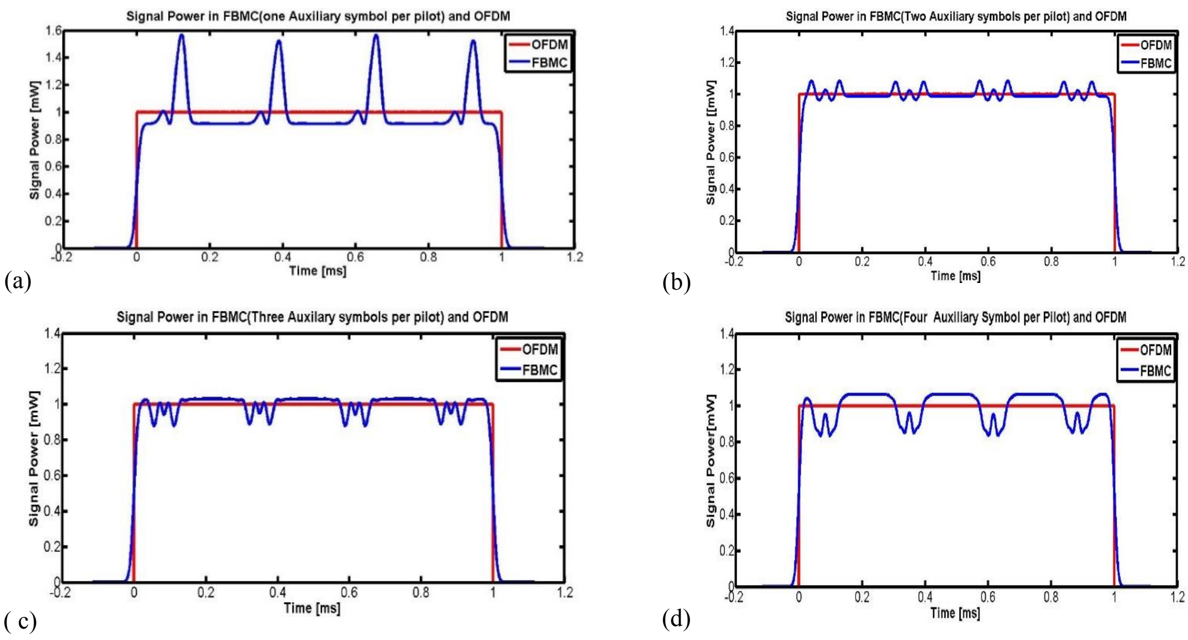

Figure 4. (a), (b), (c) and (d) are the signal power of FBMC and OFDM with number of Auxiliary symbols per pilot from *mono-* to *tetra*

Various performance metrics such as transmission power, throughput and BER are computed for Multi carrier modulations such as OFDM, FBMC using the computation model shown in Figure 3. While implementing this model higher order Quadrature Amplitude Modulation (QAM) like 4-where FNA in $P_{D,FNA}$ denotes FBMC based number of auxiliary symbols per pilot, and it varies from 1 to 4. P_n is the noise power. FBMC is operated in real domain, so the noise power P_n is reduced by a factor of 2.

If FBMC uses a greater number of subcarriers, the available transmission power must be dispersed over a wider bandwidth.

As a result, it reduces each symbol transmission power while keeping the noise power constant, resulting in a poor SNR.

The power required to transmit OFDM and FBMC are evaluated by varying the Auxiliary symbols per pilot from *mono-* to *tetra-* are shown in Figure.4.

If the number of auxiliary symbols is increased from mono- to tetra-the available power to transmit the data symbols also increases. Then the number of data symbols reduced, but the auxiliary symbol power can be significantly reduced, shown in Table 1.

Throughput computation

Throughput is computed by considering only one auxiliary symbol per pilot with various interpolation methods. In Moving block average-based interpolation, the average of all pilot estimates is considered within a time frequency range, whereas in linear interpolation the three closest pilot estimates are considered. The wireless channel is highly correlated in both frequency and time domain. Due to this, moving block average interpolation is better than the linear interpolation by nearly 1.7 dB SNR.

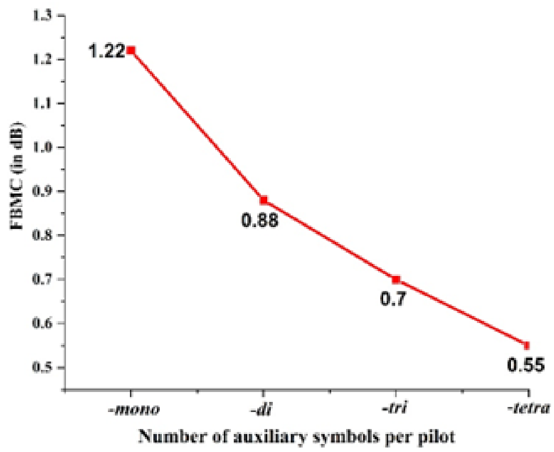

Figure 5: Shift of SNR for FBMC with auxiliary symbols per pilot from *mono-* to *tetra-*

Based on the relationships given by Eq.11 and Eq.12, the SNR of FBMC and OFDM are calculated by varying auxiliary symbols per pilot from 1 to 4 and comparison with OFDM is shown in Fig. 5.

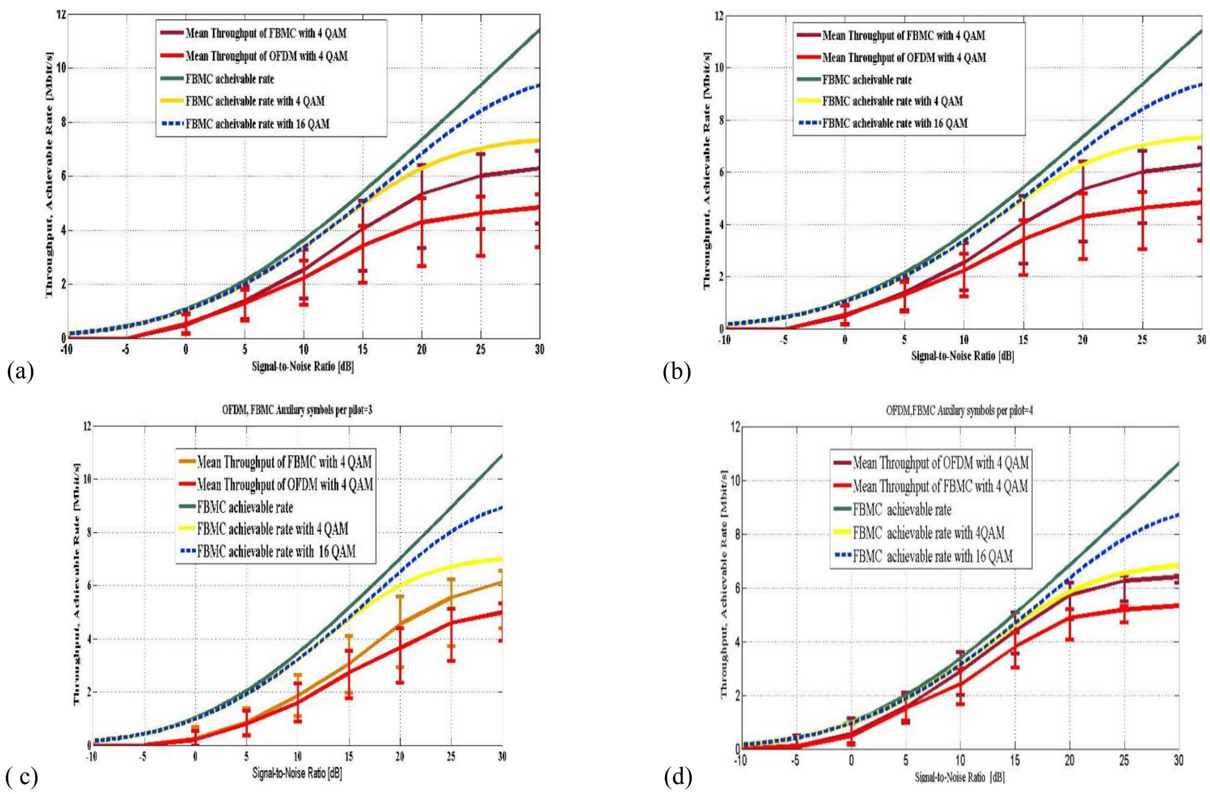

Figure 6: (a), (b), (c) and (d) are the throughput achievable rate for FBMC and OFDM with number of Auxiliary symbols per pilot from *mono-* to *tetra-*

From Figure 5 compared to OFDM, in FBMC an earlier shift of 1.22dB is observed for one auxiliary symbol per pilot. Similarly, an earlier shift of 0.88 dB is observed for two auxiliary symbols per pilot, an earlier shift of 0.7 dB is observed for three auxiliary symbols per pilot, and earlier shift of 0.55 dB is observed for four auxiliary symbols per pilot. Throughput is calculated by varying SNR and the effect of channel capacity for the measured throughput is shown in Figure. 6. For the computation of throughput such as mean throughput (average Throughput), achievable throughput (maximum throughput) the computational model is shown in Figure 3.

For a low SNR, the throughput is increased. The increased throughput of data symbols compensates the loss of throughput for few pilot symbols. Therefore, using multiple auxiliary symbols per pilot performs better than having one auxiliary symbol per pilot.

BER computation

The BER performance of OFDM is evaluated with interference cancellation and shown in Figure 7. To improve the channel estimation accuracy pilot to data power offset of P_A/P_D =2 is considered.

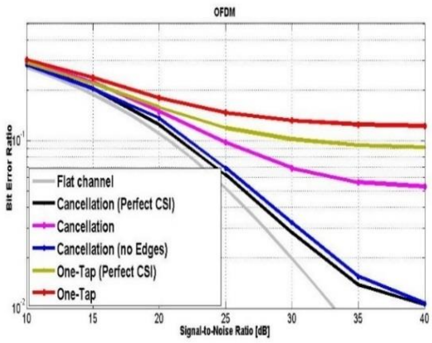

(a)

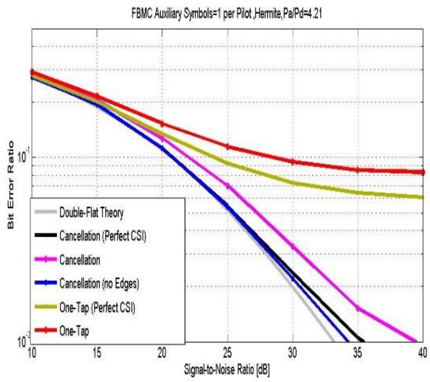

(b)

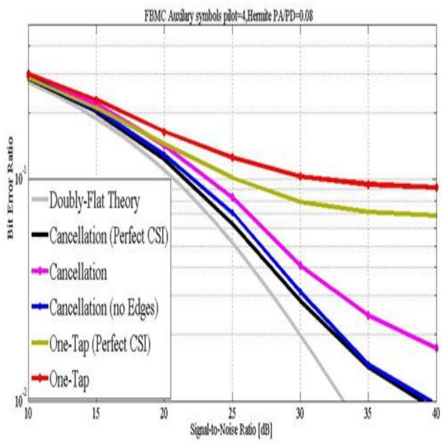

(c)

Figure 7:(a) BER performance of OFDM with interference cancellation; (b) BER performance of FBMC with interference cancellation with *mono*-Auxiliary symbols per pilot; (c) BER performance of FBMC with interference cancellation with *tetra*-Auxiliary symbols per pilot.

The performance of one Tap equalizer is poor if the interference is added to the noise. BER is computed, by excluding the time-frequency position close to the edge, i.e only points which are at the center of the frame are considered. Better BER performance (6dB) is obtained for interference cancellation with Perfect CSI (Channel State Information), and it is close to flat channel response. The proposed Auxiliary symbol approach for FBMC is compared with OFDM and plotted in Figure.7. Only locations in the middle of the frame are taken into consideration for computing BER, while time-frequency positions near the edge are excluded. Perfect CSI (Channel State Information) results in better BER performance (6dB) for interference cancellation, and the channel response is nearly flat for the FBMC with proposed auxiliary symbol approach. By varying the number of pilots from *mono to tetra* for FBMC, BER is computed and shown in Figure.8.

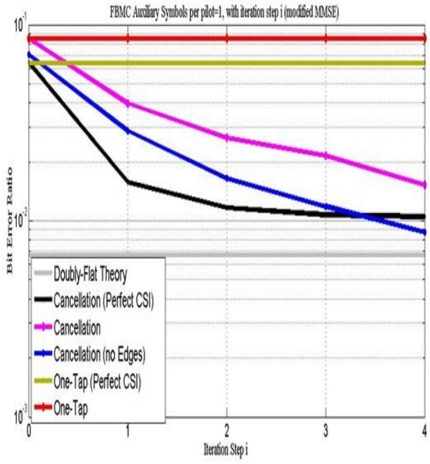

(a)

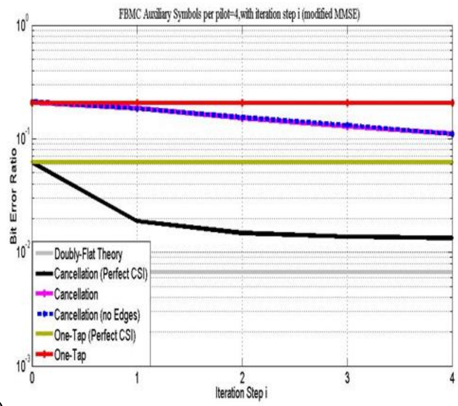

(b)

Figure 8: BER performance of FBMC with Modified MMSE(Iterated MMSE) and with *mono*-Auxiliary symbols per pilot (b) BER performance of FBMC with Modified MMSE(Iterated MMSE)and *tetra*- Auxiliary symbols per pilot

BER is also computed by performing a number of Montecarlo simulations and plotted and shown in Figure 8(a-b). From the Figure. 8. the BER performance of FBMC using the auxiliary symbol channel estimation method with auxiliary symbols per pilot from *mono*- to *tetra*-, it is observed that by employing *tetra*-auxiliary symbols per pilot, the interference cancellation method obtains 3 dB less performance for the least $(\frac{P_A}{P_D})$ power offsets i.e only 0.08. FBMC shows better performance because of more power for data symbols and less channel-induced interference than OFDM.

By increasing the number of iteration steps from *mono*- to *tetra*- BER is reduced to 0.2 dB to 0.1 dB for interference cancellation scheme. If the number of iterations is increased the performance of BER is improved which is shown in Figure 7(a-b). Imaginary interference cancellation based on MMSE method achieves better performance compared to iteration $i = 1$ to $i = 4$. This is achieved only due to the cancellation of imaginary interference by increasing the auxiliary pilot symbols from mono to tetra.

IV. CONCLUSIONS

The proposed channel estimation and interference cancellation are suitable to any physical layer modulations such as OFDM and FBMC. To cancel the imaginary interference and to estimate the channel, auxiliary symbols are transmitted along with the pilot. When one auxiliary symbol is transmitted per pilot, the power offset, and transmission power enhancement are observed. The number of symbols allotted to data can be decreased by transmitting multiple Auxiliary symbols per pilot, while the power required to transmit the signal and power offsets can be reduced. When the SNR is low, the throughput gain of more data symbols compensates for the throughput loss of a fewer number of data symbols. As a result, using numerous symbols per pilot outperforms using only one auxiliary symbol. Due to the availability of more power for data symbols in FBMC, the BER performance is better than OFDM. The performance of the proposed MMSE channel estimation scheme is close to the ideal channel because it is designed to deal with large delay spread and Doppler spread channels. The auxiliary symbol-based channel estimation approach outperforms the conventional process and has the added benefit of higher throughput.

REFERENCES

[1] 3GPP TS 36.214: version10.1.0 Release 10. *Physical layer: Measurements*. 2011

[2] Ghosh, Sudipta, and Ankit Bass, "Implementation of digital video broadcasting-terrestrial (DVB-T) using orthogonal frequency division multiplexing (OFDM) on physical media dependent sub layer," *Int. J. Comput. Appl.*, vol. 44, no. 22, pp. 20–25, 2012.

[3] Pan, Lebing, Jun Ye, and Xiaobing Yuan, "Spectral precoding for out-of-band power reduction under condition number constraint in OFDM-based systems," *Wireless Personal Communications,* vol. 95, no. 2, pp. 1677–1691, 2017. DOI: 10.1007/s11277-016-3874-8

[4] Tanda, Mario. "Performance analysis of FBMC/OQAM systems in frequency-selective channels." *Digital Signal Processing 134* (2023): 103935.

[5] Pishvaei, Seyed Mahmoud, Behzad Mozaffari Tazehkand, and Jafar Pourrostam. "Design and performance evaluation of FBMC-based orthogonal time–frequency space (OTFS) system." *Physical Communication* 53 (2022): 101723.

[6] Gregoratti, David, and Xavier Mestre, "Uplink FBMC/OQAM-based multiple access channel: Distortion analysis under strong frequency selectivity," *IEEE Transactions on Signal Processing*, vol. 64, no. 16, pp. 4260–4272, 2016.

[7] Kim, Chanhong, Yeo Hun Yun, Kyeongyeon Kim, and Ji-Yun Seol, "Introduction to QAM-FBMC: From waveform optimization to system design," *IEEE Communications Magazine*, vol. 54, no. 11, pp. 66–73, 2016. DOI: 10.1109/MCOM.2016.1600384CM

[8] Mahama, Sumaila, Yahya Jasim Harbi, Alister G. Burr, and David Grace, "Design and Convergence Analysis of an IIC-based BICM-ID Receiver for FBMC-QAM Systems," *IEEE Open Journal of the Communications Society*, vol. 1, pp. 563–577, 2020. DOI: 10.1109/OJCOMS.2020.2992314

[8] Sim, Dongkyu, and Chungyong Lee, "A MIMO receiver with two-dimensional ordering for maximum likelihood detection in FBMC-QAM," *IEEE Communications Letters*, vol. 21, no. 7, pp. 1465–1468, 2017. DOI: 10.1109/LCOMM.2017.2689003

[9] Kwon, Beom, Seonghyun Kim, and Sanghoon Lee, "Scattered reference symbol-based channel estimation and equalization for FBMC-QAM systems," I*EEE Transactions on Communications*, vol. 65, no. 8, pp. 3522–3537, 2017. DOI: 10.1109/TCOMM.2017.2710310

[10] Cheng, Xing, Dejun Liu, Chen Wang, Song Yan, and Zhengyu Zhu, "Deep learning-based channel estimation and equalization scheme for FBMC/OQAM systems," I*EEE Wireless Communications Letters*, vol. 8, no. 3, pp. 881–884, 2019. DOI: 10.1109/LWC.2019.2898437

[11] Fuhrwerk, Martin, Sanam Moghaddamnia, and Jürgen Peissig, "Scattered pilot-based channel estimation for channel adaptive FBMC-OQAM systems," *IEEE Transactions on Wireless Communications*, vol. 16, no. 3, pp. 1687–1702, 2017. DOI: 10.1109/TWC.2017.2651806

[12] Lee, Taehyun, Dongkyu Sim, Bongsung Seo, and Chungyong Lee, "Channel estimation scheme in oversampled frequency domain for FBMC-QAM systems based on prototype filter set," *IEEE Transactions on Vehicular Technology*, vol. 68, no. 1, pp. 728–739, 2018. DOI: 10.1109/TVT.2018.2885078

[13] Jeon, Donghyun, Seonghyun Kim, Beom Kwon, Hojae Lee, and Sanghoon Lee, "Prototype filter design for QAM-based filter bank multicarrier system," *Digital Signal Processing*, vol. 57, pp. 66–78, 2016. DOI: 10.1016/j.dsp.2016.05.002

[14] Bazzi, Jamal, Petra Weitkemper, and Katsutoshi Kusume, "Power efficient scattered pilot channel estimation for FBMC/OQAM," In *SCC 2015; 10th International ITG Conference on Systems, Communications and Coding*, VDE, pp. 1–6, 2015.

[15] J. F. Du and S. Signeel, "Novel preamble-based channel estimation for OFDM/OQAM systems," in *Proceedings 2009 IEEE International Conference on Communications*, Dresden, Germany, pp. 1–6, June 2009.

[16] E. Kofidis and D. Katselis, "Improved interference approximation method for preamble-based channel estimation in FBMC/OQAM," in *Proceedings IEEE European Signal Process.Conference*, Barcelona, Spain, pp. 1603–1607, September 2011.

[17] H. Wang, W. C. Du, and L. W. Xu, "Novel preamble design for channel estimation in FBMC/OQAM systems," *KSII Transactions on Internet and Information Systems*, vol. 10, no. 8, pp. 3672–3688, 2016.

[18] Kwon, Beom, Seonghyun Kim, and Sanghoon Lee, "Scattered reference symbol-based channel estimation and equalization for FBMC-QAM systems," *IEEE Transactions on Communications*, vol. 65, no. 8, pp. 3522–3537, 2017. DOI: 10.1109/TCOMM.2017.2710310

[19] Han, Hyungsik, Namshik Kim, and Hyuncheol Park, "Design of QAM- FBMC waveforms considering MMSE receiver," *IEEE Communications Letters*, vol. 24, no. 1, pp. 131–135, 2019. DOI: 10.1109/LCOMM.2019.2952375

[20] Xiaoli, Ma, G. B. Giannakis, and Shuichi Ohno. "Optimal training for block transmissions over doubly selective wireless fading channels." *IEEE Transactions on Signal Processing* 51.5 (2003): 1351–1366.

[21] Lee, Taehyun, et al. "Channel estimation scheme in oversampled frequency domain for FBMC-QAM systems based on prototype filter set." *IEEE Transactions on Vehicular Technology* 68.1 (2018): 728–739.

[22] Hassan, Beenish, et al. "Adaptive refined random orthogonal matching pursuit algorithm for FBMC/OQAM MIMO framework." *Alexandria Engineering Journal* 87 (2024): 319–328.

[23] Saideh, Michel, Marion Berbineau, and Iyad Dayoub, "On doubly selective channel estimation for FBMC-OQAM using the LMMSE filter for future railway communications," In *2018 16th International Conference on Intelligent Transportation Systems Telecommunications (ITST)*, IEEE, pp. 1–6, 2018. DOI: 10.1109/ITST.2018.8566706

[24] Padmavathi, Thodupunoori, Kusma Kumari Cheepurupalli, and R. Madhu. "Analysis of Multi Carrier Modulation Techniques for 5G Physical Layer Communications Estimation of KPI." *Journal of Scientific & Industrial Research* 81.11 (2022): 1224–1232. http://nopr.niscpr.res.in/handle/123456789/60912

[25] Liu, Wenfeng, *et al*. "Preamble-based channel estimation for OQAM/FBMC systems with delay diversity." *IEEE Transactions on Wireless Communications* 19.11 (2020): 7169–7180.

[26] Chen, Da, Rui Wang, and Tao Jiang. "Channel estimation and pilot symbol optimization based on intrinsic interference utilization for OQAM/FBMC systems." *IEEE Transactions on Signal Processing 69* (2021): 4595–4606.

[27] Wang, Ying, *et al*. "Bi-orthogonality recovery and MIMO transmission for FBMC Systems based on non-sinusoidal orthogonal transformation." *Signal Processing* (2024): 109427.

[28] Rosenkilde, Johan, and Arne Storjohann, "Algorithms for simultaneous Hermite–Padé approximations," *Journal of Symbolic Computation*, vol. 102, pp. 279–303, 2021. DOI: 10.1016/j.jsc.2019.07.026

[29] Jeannerod, Claude-Pierre, Vincent Neiger, Éric Schost, and Gilles Villard, "Computing minimal interpolation bases," *Journal of Symbolic Computation*, vol. 83, pp. 272–314, 2017. DOI: 10.1016/j.jsc.2016.11.015

[30] Nissel, Ronald, and Markus Rupp, "On pilot-symbol aided channel estimation in FBMC-OQAM," In *2016 IEEE International conference on acoustics, speech and signal processing (ICASSP)*, IEEE, pp. 3681–3685, 2016.

[31] Cui, Wenjia, Daiming Qu, Tao Jiang, and Behrouz Farhang-Boroujeny, "Coded auxiliary pilots for channel estimation in FBMC-OQAM systems," *IEEE Transactions on Vehicular Technology*, vol. 65, no.5, pp. 2936–2946, 2015. DOI: 10.1109/TVT.2015.2448659

[32] Kong, Dejin, Xing Zheng, Yue Zhang, and Tao Jiang, "Frame repetition: A solution to imaginary interference cancellation in FBMC/OQAM systems," *IEEE Transactions on Signal Processing*, vol. 68, pp. 1259–1273, 2020. DOI: 10.1109/TSP.2020.2971185

[33] Choi, Jeong-Min, Youngho Oh, Hakju Lee, and Jong-Soo Seo, "Pilot-aided channel estimation utilizing intrinsic interference for FBMC/OQAM systems," *IEEE Transactions on Broadcasting*, vol. 63, no. 4, pp. 644–655, 2017. DOI: 10.1109/TBC.2017.2711143

[34] Singh, Prem, Himanshu B. Mishra, Aditya K. Jagannatham, and Kasturi Vasudevan, "Semi-blind, training, and data-aided channel estimation schemes for MIMO-FBMC-OQAM systems," *IEEE Transactions on Signal Processing*, vol. 67, no. 18, pp. 4668–4682, 2019. DOI: 10.1109/TSP.2019.2925607

T. Padmavathi did M.Tech in Systems in signal Processing currently pursuing Ph.D in the field of Wireless Communications & Signal processing, from JNTU, Kakinada. She is currently working as Sr. Assistant Professor with the Department of Electronics and Communication Engineering, CVR College of Engineering, Ibrahimpatnam, Hyderabad, India. She has published papers in the field of MIMO, Channel Estimation in the reputed Journals

Kusma Kumari Cheepurupalli has done Ph.D in the field of Signal processing and Communications from Andhra University, Visakhapatnam. She did her M.Tech project in Naval Science Technological Laboratory, Vishakhapatnam. She is the Principal Investigator for the project titled ‘Robust Signal Processing Techniques for RADAR/SONAR Communications”, granted by DST under Women Scientist Scheme. She has got 4 best papers awards in the various Conferences. She has got more than 25 papers in the reputed journals. She has 3 patent grants and Co-author for the Text book “Semiconductor Physics and Devices”, published by Deccan International Publisher. Currently working as Associate Professor in Gayatri Vidya Parishad College of Engineering (Autonomous), Visakhapatnam.

Madhu Ramarakula was born in Warangal district, INDIA in 1980. He received the B.E (Bachelor of Engineering) degree in Electronics and Communication Engineering from Osmania University, Hyderabad, India, in 2003 and M.Tech degree in Communication Systems from Jawaharlal Nehru Technological University Hyderabad, India, in 2009. He received his Ph.D degree in Electronics and Communication Engineering from Andhra University, Visakhapatnam, India, in 2014. He is presently working as an Assistant Professor in the Department of Electronics and Communication Engineering, University College of Engineering Kakinada (A), JNTUK Kakinada, India. He has 10 years of teaching experience. He has published more than 40 research papers in various reputed national and international Journals and conferences. His research interests include Mobile and Cellular Communications, Antennas, Satellite communications and GNSS. He is a member of IEEE.